Image Contrast Using the Secondary and Tertiary Eigenvectors in Diffusion Tensor Imaging

J. Zhang[1,2], P. C. van Zijl[1,3], S. Mori[1,3]

[1]Radiology, Johns Hopkins University School of Medicine, Baltimore, MD, United States, [2]Biomedical Engineering, Johns Hopkins University, Baltimore, MD, United States, [3]F.M. Kirby Research Center for Functional Brain Imaging, Kennedy Krieger Institute, Baltimore, MD, United States

Introduction

In diffusion tensor imaging (DTI), diffusion measurements are fitted into a tensor model. Each diffusion tensor can be equivalently represented by its three eigenvectors (V_1, V_2 and V_3) and associated eigenvalues (λ_1, λ_2, λ_3 of descending magnitude). Various anisotropy indices have been proposed to measure anisotropy of water diffusion, and V_1 has been used to reconstruct white matter structures. Even though DTI is an over-simplification for complex anatomical structures, the whole information provided by DTI has not been fully utilized in routine studies. Several studies have shown that V_2 can provide additional information [1, 2]. In this study, we investigated DTI-based contrasts that reflect properties of V_2 and V_3. The relationships between these contrasts and underlying neuroanatomy are investigated using a mouse brain model. Their usefulness in studying cellular events during brain development and tissue segmentation is assessed. Finally, the contrasts are also studied in human brains to assess the usefulness of these contrasts for clinical studies.

Methods

Four anisotropy indices were investigated in this study, and their definition are shown on the right, where $D_{av} = (\lambda_1 + \lambda_2 + \lambda_3)/3$, and the function *min* returns the smallest inputs. A digital phantom was constructed to study the characteristics of the four anisotropy indices. Depending on the relative magnitude of the three eigenvalues, diffusion tensor can have tubular, planar or spherical shapes [3]. Tubular tensors have high CL values, and planar tensors have high CP values [3]. Tensors that satisfy $\lambda_1 >> \lambda_2 >> \lambda_3$ have high SI values. V_1 estimation is robust when CL is high. V_2 and V_3 estimations are robust when SI and CP are high, respectively. We combined V_1 with CL, V_2 with SI and V_3 with CP to generate V_1·CL, V_2·SI and V_3·CP images. Human and mouse brain images were acquired in previous studies and reanalyzed here [4, 5]. Monte Carlo simulations were performed on the phantom to examine the effect of noise on the eigenvectors and anisotropy indices as described before [6].

$$FA = \frac{\sqrt{(\lambda_1-\lambda_2)^2+(\lambda_1-\lambda_3)^2+(\lambda_2-\lambda_3)^2}}{\sqrt{2(\lambda_1^2+\lambda_2^2+\lambda_3^2)}}$$

$$CL = \frac{\lambda_1-\lambda_2}{\lambda_1} = 1-\frac{\lambda_2}{\lambda_1},\ CP = \frac{\lambda_2-\lambda_3}{\lambda_1}$$

$$SI = \min\left\{\frac{\lambda_1-\lambda_2}{D_{av}}, \frac{\lambda_2-\lambda_3}{D_{av}}\right\}$$

Results and Discussion

These new contrasts were first examined using well known anatomical structures. For large fiber bundles in adult mouse brain, the measured anisotropy values (high CL, low SI and CP, table 1) agree with the highly coherent fiber orientations inside these structures. In comparison, the cortical regions have low CL, SI and CP. Mouse cerebellum contains parallel fibers and Purkinje fibers in an orthogonal configuration. Parallel fibers outnumber Purkinje fibers. In DTI results (Fig. 1), V_1·CL reveals that the tissue orientation in the cerebellar cortex is along the orientation of the parallel fibers (red, medial-lateral). V_2·SI shows that the V_2s in the cerebellar cortex are mostly along the orientation of the Purkinje fiber (green, anterior-posterior). In embryonic mouse cerebral cortex, the V_1·CL and V_3·CP contrasts provide better tissue differentiation than V_1·FA (results not shown here). The morphology of the cortical plate and intermediate zone can be clearly appreciated in the V_1·CL and V_3·CP images. These results show that the new contrasts can reveal additional anatomical information for tissue differentiation.

	FA	CL	SI	CP
Optic nerve	0.77±0.07	0.76±0.07	0.13±0.08	0.06±0.04
Anterior commissure	0.85±0.07	0.82±0.07	0.22±0.10	0.10±0.04
Corpus callosum	0.79±0.08	0.76±0.11	0.20±0.13	0.10±0.10
Motor cortex	0.19±0.03	0.11±0.05	0.08±0.03	0.09±0.05
Sensory cortex	0.14±0.03	0.14±0.05	0.09±0.04	0.10±0.04

Table 1: Average FA, CL, SI and CP values of several white matter and gray matter structures in an ex vivo mouse brain.

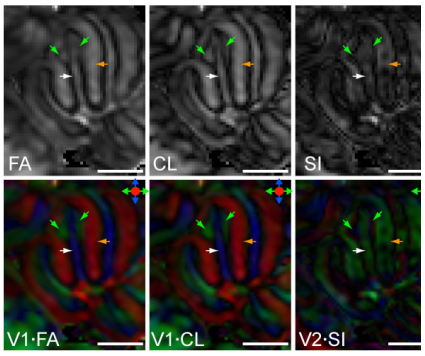

Fig. 1: Images of adult mouse cerebellum generated using the new contrasts showing the cerebellar cortex (orange arrows) and cerebellar white matter (white arrows). Scale bars = 1 mm.

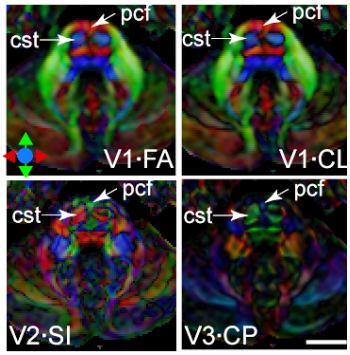

Fig. 2: Images of human pons in a healthy volunteer. Abbreviations are: cst: corticospinal tract; pcf: pontine crossing fiber. Scale bar = 30 mm.

The contrasts were applied to human brains. In the human pons (Fig. 2), V_1·CL image shows that the regions of the corticospinal tract (cst) are dominated by longitudinal fibers (blue, superior-inferior). Surrounding the corticlspinal tracts are pontine crossing fibers (pcf), which are transverse fibers (red, medial-to-lateral). The longitudinal and transverse fibers are orthogonal to each other. In the V_2·SI image, the corticospinal tract regions are red, revealing the existence of transverse pontine crossing fibers in the region. In a patient with paraventricular leukomalacia, V_1·CL shows that the longitudinal fibers were damaged and were outnumbered by the transverse fibers (results not shown here). V_2·SI shows that residual longitudinal fibers still exist.

These results demonstrate the usefulness of these contrasts in diagnosis of white matter lesions. These contrasts also have limitations. For interpretation of the contrasts, *a prior* knowledge about axonal organization is imperative.

References:

1. Mamata H et al, ISMRM, Honolulu, HI, 2002.
2. Hirsch JG et al, ISMRM, Toroto, Cananda, 2003.
3. Westin CF et al, Med Image Anal 2002;6(2):93-108.
4. Wakana, S. et al, Radiology 2004;230(1):77-87.
5. Zhang, J. et al, Neuroimage 2003;20(3):1639-1648.
6. Pierpaoli, C. et al, MRM 2000;44(1): 41-50.